Photoconductivity on nanocrystalline ZnO/TiO_2 thin films obtained by sol-gel

G. Valverde-Aguilar[1], J. A. García-Macedo [1*], R. Juárez-Arenas[1]

1. Departamento de Estado Sólido. Instituto de Física, Universidad Nacional Autónoma de México. México D.F. C.P. 04510

*** Contact author:**
Dr. Jorge Garcia Macedo
Instituto de Física, UNAM
Circuito de la Inv. Científica s/n
C. P. 04510. Del. Coyoacán
México, D.F.
México.
Tel. (5255) 5622–51–03
Fax (5255) 5616–15–35
E–mail: gamaj@fisica.unam.mx

ABSTRACT

In this paper we report results on the synthesis, characterization and photoconductivity behaviour of amorphous and nanocrystalline ZnO/TiO_2 thin films. They were produced by the sol–gel process at room temperature by using the spin-coating method and deposited on glass substrates. The ZnO/TiO_2 films were synthesized by using tetrabutyl orthotitanate and zinc nitrate hexahydrate as the inorganic precursors. The samples were sintered at 520°C for 1 hour. The obtained films were characterized by X-ray diffraction (XRD), optical absorption (OA), infrared spectroscopy (IR) and scanning electronic microscopy (SEM) studies. Photoconductivity studies were performed on amorphous and nanocrystalline (anatase phase) films to determine the charge transport parameters. The experimental data were fitted with straight lines at darkness and under illumination at 310 nm, 439 nm and 633 nm. This indicates an ohmic behavior. The $\phi\mu\tau$ and ϕI_0 parameters were fitted by least-squares with straight lines (nanocrystalline films) and polynomial fits (amorphous films).

KEYWORDS: Titania, zinc oxide, semiconductors, sol-gel, thin film

1. INTRODUCTION

Titanium dioxide is a non-toxic material. TiO_2 thin films exhibit high stability in aqueous solutions and no photocorrosion under band gap illumination and special surface properties. TiO_2 thin films are already widely used in the study of the photocatalysis and photoelectrocatalysis of organic pollutants [1, 2]. Photoelectrocatalytic system has received a great deal of attention due to drastically enhanced quantum efficiency [3]. By applying small bias, recombination of generated electron–hole pairs is retarded. TiO_2 has been widely used as photoelectrocatalyst for water and air purification because of high surface activity, absence of toxicity and chemical stability [4, 5]. ZnO has been reported to be photoactive for phenol and nitrophenol degradation in spite of some photocorrosion effects in the liquid–solid phase.

ZnO has been also conceived as a significant candidate for photooxidation of organic compounds and has reportedly known to be more efficient than TiO_2. The band gap energies of ZnO and TiO_2 are similar to each other (approximately 3.2eV). However, the intrinsic semiconducting characteristics of ZnO and TiO_2 are different, i. e., ZnO is a direct band gap semiconductor but TiO_2 is an indirect band gap semiconductor [6-8].

In the present work, we described the synthesis, characterization and photoconductivity behaviour of amorphous and nanocrystalline $ZnO-TiO_2$ thin films. The films were produced by the sol–gel process at room temperature by using the

Nanostructured Thin Films, edited by Geoffrey B. Smith, Akhlesh Lakhtakia,
Proc. of SPIE Vol. 7041, 70410U, (2008) · 0277-786X/08/$18 · doi: 10.1117/12.795461

spin-coating method and deposited on glass substrates. The samples were sintered at 520°C for 1 hour. The obtained films were characterized by X-ray diffraction, optical absorption, FTIR and TEM studies. Photoconductivity studies were performed on amorphous and nanocrystalline (anatase phase) films. Transport parameters were calculated.

2. EXPERIMENTAL

Glass substrates were cleaned in boiling acidic solution of sulphuric acid-H_2O_2 (4:1) under vigorous stirring for 30 minutes. They were then placed in deionized water and boiled for 30 minutes, rinsed three times with deionized water and stored in deionized water at room temperature.

All reagents were Aldrich grade. The precursor solutions for ZnO/TiO_2 films were prepared by the following method. Tetrabutylorthotitanate (8.5 ml) and diethanolamine ($NH(C_2H_4OH)_2$) (2.4 ml) which prevent the precipitation of oxides and stabilize the solutions were dissolved in 34 ml of ethanol. After stirring vigorously for 2h at room temperature, a mixed solution of deionized water (0.45 ml) and ethanol (5 ml) was added dropwise slowly to the above solution with a pipette under stirring. Finally, Tetraethyleneglycol (TEG) (5g) was added to the above solution. Then, zinc nitrate hexahydrate ($Zn(NO_3)_2{\cdot}6H_2O$) (4.26 g) was added into TiO_2 sol vigorously to obtain an uniform sol. The resultant alkoxide solution was kept standing at room temperature to perform hydrolysis reaction for 2h, resulting in the TiO_2 sol. The chemical composition of the starting alkoxide solution was $Ti(OC_4H_9)_4$: C_2H_5OH : DI H_2O : $NH(C_2H_4OH)_2$: TEG: $Zn(NO_3)_2{\cdot}6H_2O$ = 1:14.1:1:1:1.0296:0.57. The TiO_2 solution had a pH = 6.0. The ZnO/TiO2 films were prepared by the spin-coating technique. The precursor solution was placed on the glass substrates (2.5 x 2.5 cm^2) using a dropper and spun at a rate of 3000 rpm for 20 s (Figure 1).

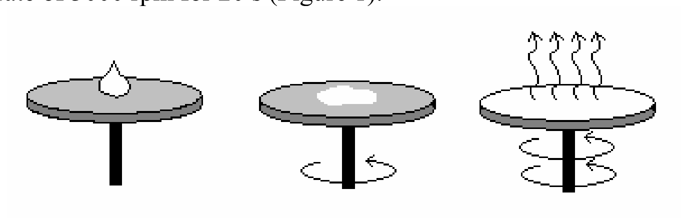

Figura 1. Spin-coating technique.

After coating, the film was dried at 100 °C for 30 min in a muffle oven and sintered at 520 °C for 1 h in a muffle oven in order to remove organic components. The procedure was repeated five times to achieve the film thickness with five layers.

UV-vis absorption spectra were obtained on a Thermo Spectronic Genesys 2 spectrophotometer with an accuracy of ±1 nm over the wavelength range of 300-900 nm. The structure of the final films was characterized by X-ray diffraction (XRD) patterns. These patterns were recorded on a Bruker AXS D8 Advance diffractometer using Ni-filtered CuKα radiation. A step-scanning mode with a step of 0.02° in the range from 1.5 to 60° in 2θ and an integration time of 2 s was used. The thickness of the films was measured using a SEM microscopy Model JSM 5200 CX at 15 kV.

For photoconductivity studies[9] silver electrodes were painted on the sample. It was maintained in a 10^{-5} Torr vacuum cryostat at room temperature in order to avoid humidity. For photocurrent measurements, the films were illuminated with light from an Oriel Xe lamp passed through a 0.25m Spex monochromator. Currents were measured with a 642 Keithley electrometer connected in series with the voltage power supply. The applied electrostatic field E was parallel to the film. Light intensity was measured at the sample position with a Spectra Physics 404 power meter (Figure 2).

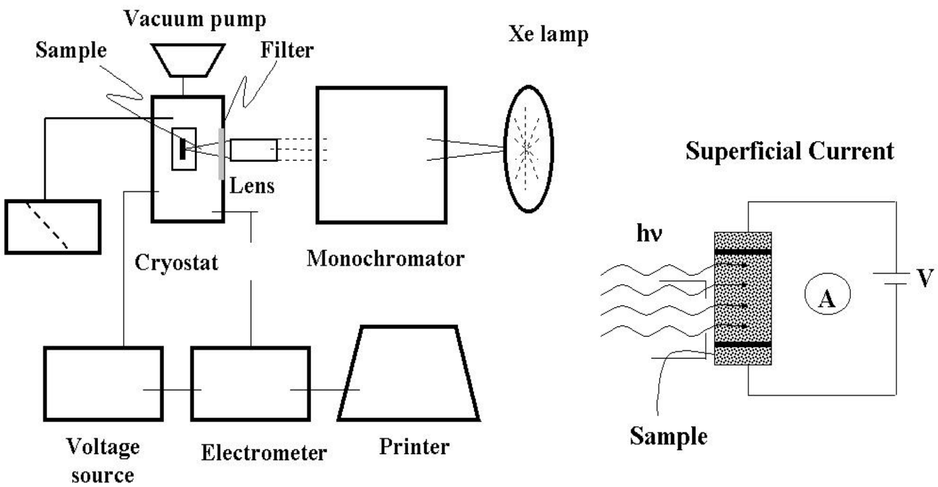

Figure 2. Schematic diagram of the photoconductivity technique. Superficial current was produced on the thin film when an electric field was applied to it.

3. RESULTS AND DISCUSSION

3.1 SEM measurements. The thickness of the films was measured by SEM technique. Figure 3 shows the SEM image for amorphous film (before calcination), the thickness is 0.19 ± 0.01 μm. After, the film was calcined at 520 °C for 1 hour to obtain a nanocrystalline phase. Figure 4 (a) shows the SEM image for nanocrystalline films, the thickness is 2.38 ± 0.33 μm; (b) it is an amplification of the nanocrystalline film showing five layers deposited on the glass substrate. The thickness for nanocrystalline film is bigger than that from amorphous film. It suggests that the calcination process swelling the layers deposited onto the substrate.

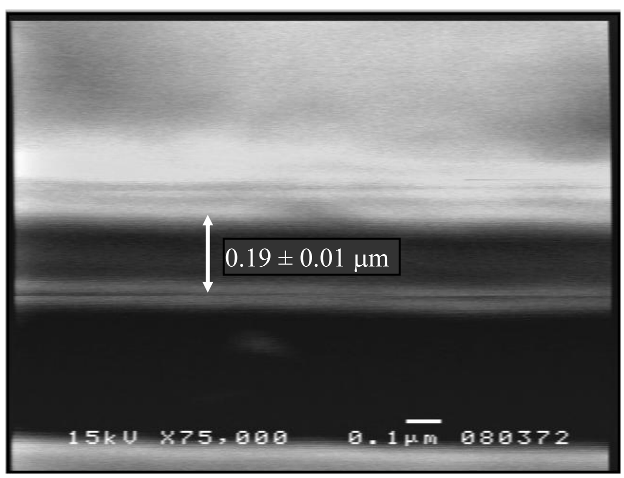

Figure 3. Cross-sectional SEM image of amorphous ZnO/TiO_2 film.

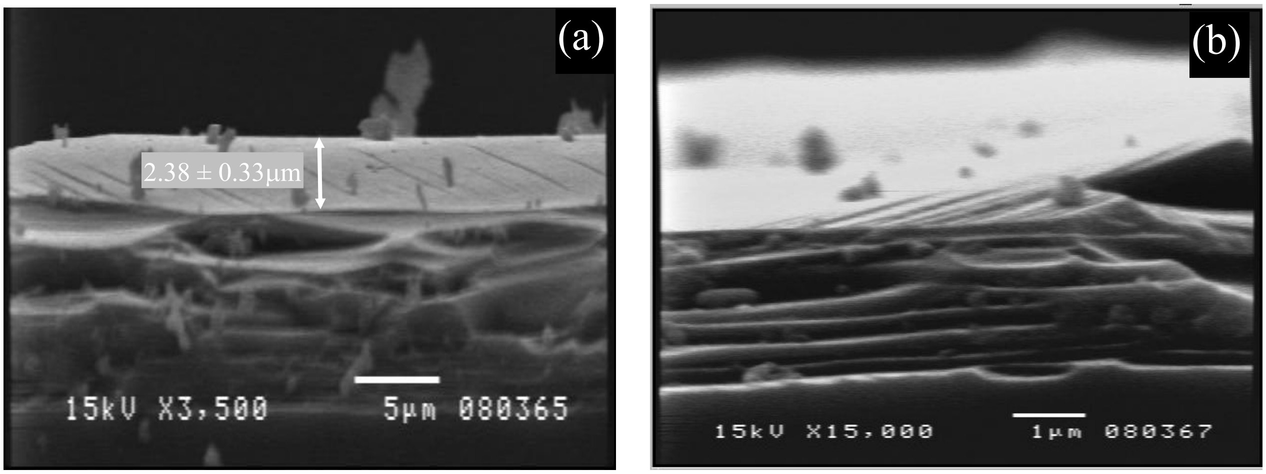

Figure 4. (a) Cross-sectional SEM image of nanocrystalline ZnO/TiO_2 film sintered at 520 °C for 1 h. (b) It is an amplification of image (a) which shows five layers deposited on the glass substrate.

3.2 Optical absorption. Figure 5 shows the optical absorption spectra of the nanocrystalline ZnO/TiO_2 thin films taken at room temperature in the range of 300-900 nm. The absorption spectrum of the amorphous film does not exhibit any band (gray line). The spectrum of the film calcined at 520 °C for 1 hour (black line) shows an absorption band A located at 315 nm.

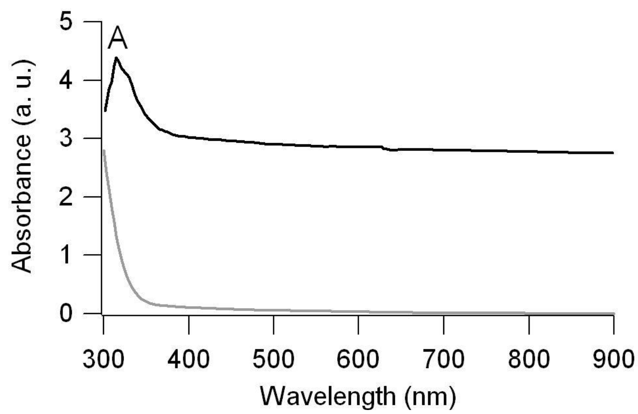

Figure 5. Absorption spectra of the ZnO/TiO_2 thin films. The spectrum for amorphous film corresponds to the gray line, and the nanocrystalline film sintered at 520 °C for 1 h corresponds to the black line.

3.3 X-ray diffraction. The X-ray diffraction patterns of the crystalline ZnO/TiO_2 films are presented in Figure 6. It is evident that the films calcined at 520 °C for 1 h exhibit very good crystallization that corresponds to anatase form of titanium dioxide formed by employing the sol-gel procedure. Wurtzite phase was not detected, that means the anatase phase is the dominant phase. The diffraction peaks located at 2θ = 25.38, 37.88, 48.08, 54.00, 54.98 and 62.84 can be indexed as (101), (004), (200), (105), (211) and (204) respectively. The position of the diffraction peaks in the film is in good agreement with those given in ASTM data card (#21-1272) for anatase form. A pure anatase phase is considered to achieve the larger surface area, which is necessary to obtain higher photoactivity[10]. The average nanocrystalline size calculated using the diffraction peak [101] from Scherer´s formula [11] was of 67.7 nm.

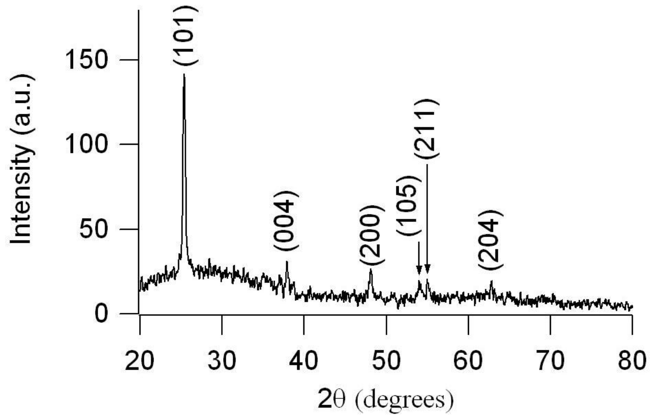

Figure 6. XRD pattern at high angle of the crystalline ZnO/TiO_2 film sintered at 520 °C for 1 h.

3.4 FTIR spectra. Figure 7 shows FTIR spectra of amorphous and nanocrystalline ZnO/TiO_2 films. For both samples, the modes observed at 411 cm^{-1}, 409 cm^{-1} agree well with the already reported values of bulk ZnO[12, 13] corresponding to the A_1 and E_1 species. The peaks at 471cm^{-1}, 476 cm^{-1} are due to the ZnO stretching mode[14]. In addition to the ethyl groups, isopropyl groups, the bands located at 2300-2900 cm^{-1} are C-H mode[15].

The spectrum 7 (a) shows the presence of OH groups (ν_{OH} at 3342 cm^{-1}, δ_{OH} at 1647 cm^{-1}), that probably belong to Ti-OH bonds as well as to the absorbed water[16]. The bands at 1348, 1454 and 2864 cm^{-1} correspond to the C-H vibrations, while the band centered at 1252 cm^{-1} originates in the C-O-C bond of TEG[16]. The band seen at 1558 cm^{-1} is due to a C = O bond. The solvent ethanol is present in the as-deposited film (ν_{OH} at 3222 cm^{-1}, $\nu_{C\text{-}O}$ at 1063 cm^{-1}). In the spectrum 7 (b), the bands around 438 cm^{-1} and 455 cm^{-1} correspond to the $\nu_{Ti\text{-}O\text{-}Ti}$ stretching vibration in the anatase phase[15, 17]. It can be seen that small amount of ethanol is present in the sintered film ($\nu_{C\text{-}O}$ at 1072 cm^{-1}). Table 1 contains the bands of amorphous and nanocrystalline ZnO/TiO_2 films and their description.

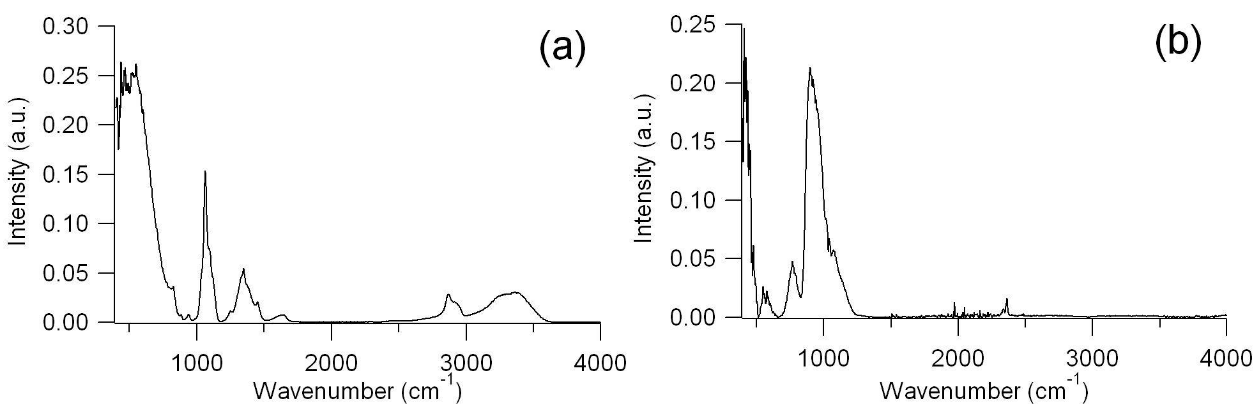

Figure 7. FTIR spectra of (a) amorphous ZnO/TiO_2 film, and (b) nanocrystalline ZnO/TiO_2 film sintered at 520 °C for 1 h.

Table 1. IR frequencies [in cm^{-1}], of the amorphous and nanocrystalline ZnO/TiO_2 films.

Amorphous	Crystalline	description
$\bar{\nu}_{exp}$ (cm^{-1})	$\bar{\nu}_{exp}$ (cm^{-1})	
411	409	E_1 (ZnO)
——	438	$\nu_{Ti-O-Ti}$ (anatase)
471	476	ZnO stretching
575	575	A_1(LO) (ZnO)
827	——	ZnO
897	897	ZnO
1063	1072	ν_{C-O} (Ethanol)
1252	——	C–O–C bond of TEG
1348	——	δ_{CH2}
1396	——	NO_3
1454	——	δ_{CH3}
1558	——	C=O
1647	——	δ_{OH}
2361	2363	C-H stretching
2864	——	C-H stretching
3222	——	ν_{OH} (Ethanol)
3342	——	ν_{OH}

3.5 Photoconductivity studies. Usually[9] Ohm's law under light illumination is given by

$$\vec{J} = \vec{J}_{ph} + \left(\sigma_d + \sigma_{ph}\right)\vec{E}\,, \tag{1}$$

where $\vec{J}_{ph}$ is the photovoltaic current density, and σ_{ph} is the photoconductivity. When the current densities are assumed to be parallel to the electric field $\vec{E}$ Eq. (1) becomes into the next one:

$$J = \frac{q\phi l_0 \alpha I}{h\nu} + \left(\sigma_d + \frac{q\phi\mu\tau\alpha I}{h\nu}\right)E\,, \tag{2}$$

with ϕ as the quantum yield of charge carrier photogeneration, l_0 as the charge carrier mean free path, α as the sample absorption coefficient, I as the light intensity at the frequency ν of illumination, h as the Planck´s constant, and τ as the charge carriers mean lifetime. The first term is the photovoltaic transport effect, the second one is the dark conductivity $\sigma_\delta = en_0\mu$, and the third one is the photoconductivity itself.

Eq (2) can be written as:

$$J = A_1 E + J_0 \tag{3}$$

From the absorption spectrum of nanocrystalline film (Fig. 5), the illumination wavelength for photoconductivity studies were chosen: 310 nm that corresponds to the maximum absorption band (315 nm), 439 nm and 633 nm were there is no absorption. Photoconductivity results of amorphous and nanocrystalline ZnO/TiO_2 films are shown on Figure 8. Current density as function of electric applied field on the film was plotted. The experimental data were fitted by least-squares with straight lines at darkness and under illumination at 310 nm, 439 nm and 633 nm. This indicates an ohmic behaviour. The linear fit for all samples are shown in Table 1. The slope from amorphous films is bigger by one order of magnitude than that from crystalline films. This is probably due to the high content of solvents in the amorphous film, as is shown in Table 1. In both kinds of samples, when the illumination wavelength increases the slope (A_1) decreases, but they are bigger than in darkness. This fact indicates a strong photoconductive behaviour.

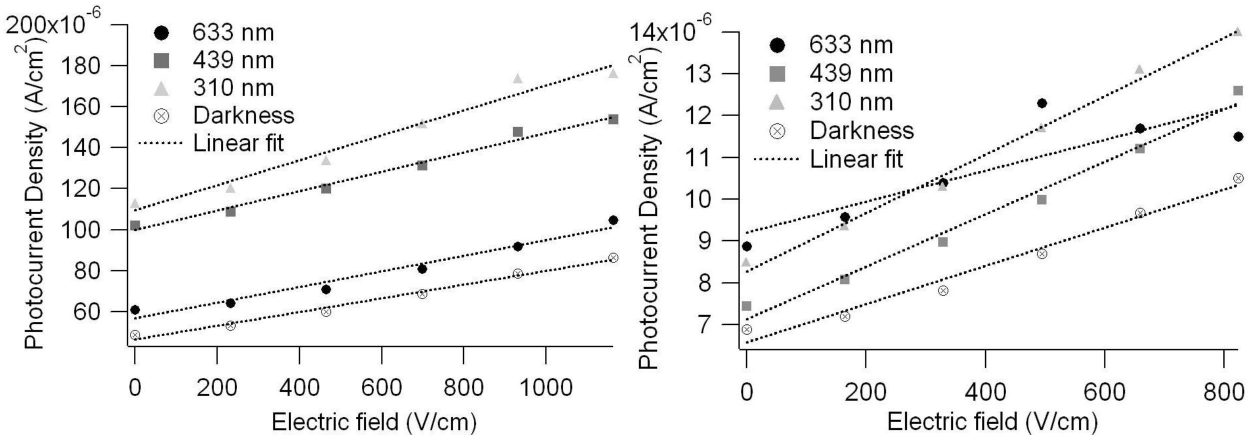

Figure 8. Photoconductivity results on (Left) amorphous ZnO/TiO_2 film, and (Right) nanocrystalline ZnO/TiO_2 film.

Table 1. Linear fittings of ZnO/TiO_2 films.

λ (nm)	Film	A_1	J_0
633	Amorphous	$3.8 \times 10^{-8} \pm 3.7 \times 10^{-9}$	$5.7 \times 10^{-5} \pm 2.6 \times 10^{-6}$
	Nanocrystalline	$3.7 \times 10^{-9} \pm 1.1 \times 10^{-9}$	$9.2 \times 10^{-6} \pm 5.5 \times 10^{-7}$
439	Amorphous	$4.8 \times 10^{-8} \pm 2.8 \times 10^{-9}$	$9.9 \times 10^{-5} \pm 1.9 \times 10^{-6}$
	Nanocrystalline	$6.3 \times 10^{-9} \pm 1.1 \times 10^{-10}$	$7.1 \times 10^{-6} \pm 2.0 \times 10^{-7}$
310	Amorphous	$6.1 \times 10^{-8} \pm 5.5 \times 10^{-9}$	$0.1 \times 10^{-5} \pm 3.8 \times 10^{-6}$
	Nanocrystalline	$7.0 \times 10^{-9} \pm 3.0 \times 10^{-10}$	$8.3 \times 10^{-6} \pm 1.5 \times 10^{-7}$
Darkness	Amorphous	$3.4 \times 10^{-8} \pm 2.0 \times 10^{-9}$	$4.6 \times 10^{-5} \pm 1.4 \times 10^{-6}$
	Nanocrystalline	$4.6 \times 10^{-9} \pm 3.5 \times 10^{-9}$	$6.6 \times 10^{-6} \pm 1.7 \times 10^{-7}$

With the equation (2), by measuring I, the dark conductivity and the conductivity under illumination at 633, 439 and 310 nm, and fitting the experimental data by the least squares method, as it is shown in Fig. 8, the photoconductive ($\phi\mu\tau$) and photovoltaic (ϕl_0) parameters were obtained (Table 2). These parameters were plotted as function of the illumination wavelength for amorphous and nanocrystalline films (Figure 9). For amorphous films, $\phi\mu\tau$ and ϕl_0 parameters reached a maximum value at 439 nm wavelength, then they decrease at 633 nm wavelength. The observed rise and decay process in the photoconductivity can be attributed to carrier detrapping effects and slow recombination of electrons and holes into the titania matrix[18]. In the nanocrystalline film, $\phi\mu\tau$ parameter decreases when the energy from illumination decreases, and it has its highest response at the maximum absorption. ϕl_0 shows a weak rise as illumination wavelength increases in these nanocrystalline films.

The $\phi\mu\tau$ and ϕl_0 parameters were fitted by least-squares with straight lines (nanocrystalline films) and polynomial fits (amorphous films) as is shown in Fig. 9. The fittings are shown in Table 3.

In spite of the titania is quite conductive under illumination[18], the coupling of anatase TiO_2 with ZnO is useful to achieve a more efficient electron-hole pair separation under illumination[19]. Electron transport is strongly affected by the efficiency with which the injected electrons can pass through the porous nanocrystalline titania film. The crystalline imperfections in the ZnO/TiO_2 matrix can influence the recombination of photogenerated holes/electron pairs. Besides this recombination can be suppressed by external electric field and the longevity of photogenerated carriers remains long[10] on the titania matrix.

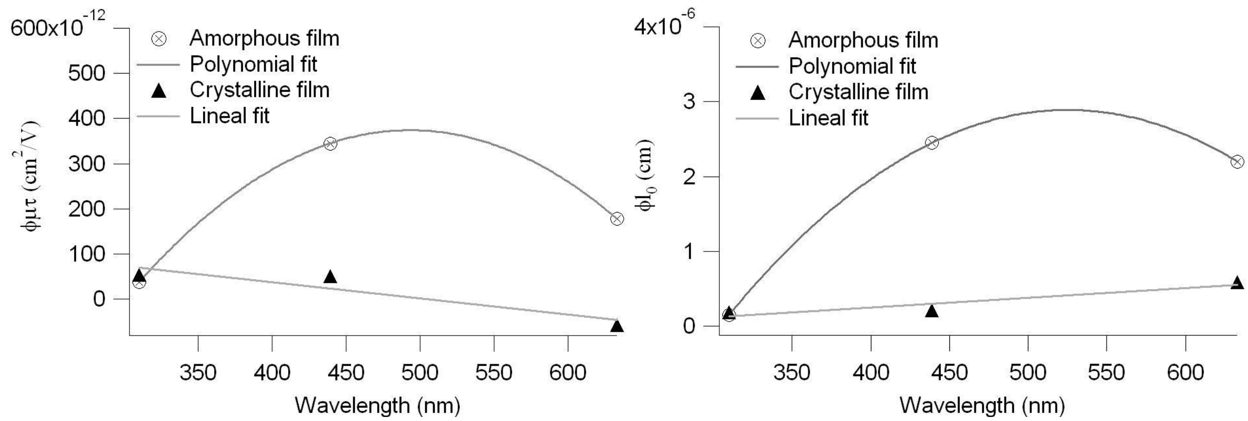

Figure 9. Photoconductive and photovoltaic parameters for amorphous and nanocrystalline films.

Table 2. Photovoltaic and photoconductive parameters of amorphous and nanocrystalline ZnO/TiO_2 film.

Sample	Parameter	633 nm	439 nm	310 nm
Amorphous ZnO/TiO_2 film	ϕl_0 (cm) $\phi\mu\tau$ (cm^2/V)	$2.20x10^{-6}$ $1.78x10^{-10}$	$2.45x10^{-6}$ $3.45x10^{-10}$	$0.15x10^{-6}$ $0.38x10^{-10}$
Nanocrystalline ZnO/TiO_2 film	ϕl_0 (cm) $\phi\mu\tau$ (cm^2/V)	$5.83x10^{-7}$ $-5.71x10^{-11}$	$2.12x10^{-7}$ $5.09x10^{-11}$	$1.84x10^{-7}$ $5.34x10^{-11}$

Table 3. Linear and polynomial fittings of $\phi\mu\tau$ and ϕl_0 parameters for amorphous and nanocrystalline ZnO/TiO_2 films.

Parameter	Amorphous	Nanocrystalline
ϕl_0	$J = -1.34 x10^{-5} + 6.2 x 10^{-8}E – 5.9 x 10^{-11}E^2$	$J = 1.3 x10^{-9} E –2.7 x 10^{-2}$
$\phi\mu\tau$	$J = -2.06 x10^{-9} + 9.9 x 10^{-12}E – 1 x 10^{-14}E^2$	$J = -3.6 x10^{-13} E + 1.8 x 10^{-10}$

4. CONCLUSIONS

Stable amorphous and nanocrystalline ZnO/TiO_2 films were obtained by sol-gel process. Photoconductivity studies on these films were done. In the amorphous sample, photoconductive parameter shows a rise and decay behaviour. It is due to the carrier detrapping effects and slow recombination of electrons and holes into the titania matrix. The photovoltaic parameter shows the rise and decay behaviour for amorphous ZnO/TiO_2 matrix and slight increase for nanocrystalline ZnO/TiO_2 matrix. $\phi\mu\tau$ and ϕl_0 parameters were fitted by least-squares with straight lines (nanocrystalline films) and polynomial fits (amorphous films). Then, the anatase phase obtained in the ZnO/TiO_2 matrix provides more stability to improve the photoconductivity.

ACKNOWLEDGMENTS

The authors acknowledge the financial supports of CONACYT 43226-F, NSF-CONACYT, PUNTA, ICYTDF and PAPIIT 116506-3. GVA is grateful for CONACYT postdoctoral fellowship. The authors are thankful to M. in Sci. Manuel Aguilar-Franco (XRD) and Jacqueline Cañetas Ortega (SEM) for technical assistance. We thank to Diego Quiterio for preparation of the samples for SEM studies.

REFERENCES

[1] R. Suarez, P. K. Nair, P.V. Kamat, "Photoelectrochemical Behavior of Bi_2S_3 Nanoclusters and Nanostructured –Thin Films", Langmuir, **14**, 3236-3241 (1998).

[2] Shaogui, Q. Xie, L. Xinyong, L. Yazi, C. Shuo, C. Guohua, "Preparation, characterization and photoelectrocatalytic properties of nanocrystalline Fe_2O_3/TiO_2, ZnO/TiO_2, and $Fe_2O_3/ZnO/TiO_2$ composite film electrodes towards pentachlorophenol degradation", Phys. Chem. Chem. Phys., **6**, 659-664 (2004).

[3] D. W. Kim , S. Lee , H. S. Jung ,J. Y. Kim , H. Shin, K. S. Hong, "Effects of heterojunction on photoelectrocatalytic properties of ZnO-TiO_2 films", International Journal of Hydrogen Energy, **32**, 3137–3140 (2007).

[4] J. Cen, X. Li, M. He, S. Zheng, M. Feng, "The effect of background irradiation on photocatalytic efficiencies of TiO_2 thin films", Chemosphere, **62** (5), 810–816 (2005).

[5] C. S. Zalazar, C. A. Martin, A. E. Cassano, "Photocatalytic intrinsic reaction kinetics. II: effects of oxygen concentration on the kinetics of the photocatalytic degradation of dichloroacetic acid", Chem. Eng. Sci, **60**, 4311–4322 (2005).

[6] G. Marci, V. Augugliaro, M. J. Lopez-Munoz, C. Martin, L. Palmisano, V. Rives et al., "Preparation, characterization and photocatalytic activity of Polycrystalline ZnO/TiO_2 systems. 2. Surface, bulk characterization, and 4-nitrophenol photodegradation in liquid–solid regime", J. Phys. Chem. B, **105**, 1033–1040 (2001).

[7] Hsu C. C., Wu N. L., "Synthesis and photocatalytic activity of ZnO/ZnO_2 composite", J. Photochem. Photobiol. A Chem, **172**, 269–274 (2005).

[8] Zhang D. K., Liu Y. C., Liu Y. L., Yang H., "The electrical properties and the interfaces of CuO/ZnO/ITO p–i–n heterojunction", Physica B, **351**, 178–183 (2004).

[9] J. García M., A. Mondragón, J. M. Hernández, J. L. Maldonado R., "Photocurrent determination of charge transport parameters in $KNbO_3:Fe^{3+}$", *Opt. Mat.* **3**, 61-64 (1994).

[10] Y. Shaogui, Q. Xie, L. Xinyong, L. Yazi, C, Shuo, C. Guohua, "Preparation, characterization and photoelectrocatalytic properties of nanocrystalline Fe_2O_3/TiO2, ZnO/TiO_2, and $Fe_2O_3/ZnO/TiO_2$ composite film electrodes towards pentachlorophenol degradation", *Phys. Chem. Chem. Phys.* **6**, 659-664 (2004).

[11] G.J. Wilson, A.S. Matijasevich, D.R.G. Mitchell, J.C. Schulz and G.D. Will, "Modification of TiO_2 for Enhanced Surface Properties: Finite Ostwald Ripening by a Microwave Hydrothermal Process", *Langmuir* **22**, 2016-2027 (2006).

[12] P. Lakshmi, K. Ramachandran, "On the Optical, Thermal, and Vibrational Properties Of Nano-ZnO:Mn, A Diluted Magnetic Semiconductor", *International Journal of Thermophysics* **28** (4), 1353-1370, 2007.

[13] N. Ashkenov, B. N. Mbenkum, C. Bundesmann, V. Riede, M. Lorenz, D. Spemann, E. M. Kaidashev, A. Kasic, M. Schubert, M. Grundmann, G. Wagner, H. Neumann, V. Darakchieva, H. Arwin, B. Monemar, "Infrared dielectric functions and phonon modes of high-quality ZnO films", *J. Appl. Phys.* **93** (1), 126-133 (2003).

[14] Z. Wang, H. Zhang, Z. Wang, L. Zhang, J. Yuan, S Yan, C. Wang, "Structure and strong ultraviolet emission characteristics of amorphous ZnO films grown by electrophoretic deposition", *J. Mater. Res.* **18** (1), 151-155 (2003).

[15] Y. Djaoued, S. Badilescu, P. V. Ashrit, D. Bersani, P. P. Lottici, "Study of Anatase to Rutile Phase Transition in Nanocrystalline Titania Films", *J. Sol-Gel Sci. & Techn.* **24**, 255–264 (2002).

[16] Y. Djaoued, S. Badilescu, P. V. Ashrit, "Low Temperature Sol-Gel Preparation of Nanocrystalline TiO_2 Thin Films", *J. Sol-Gel Sci. & Techn.* **24**, 247–254 (2002).

[17] S. Music, M. Gotic, M. Ivanda, S. Popovic, A. Turkovic, R. Trojko, A. Sekulic, K. Furic, "Chemical and micro structural properties of TiO_2 synthesized by sol-gel procedure", *Mat. Sci. and Eng. B* **47** (1), 33-40 (1997).

[18] Z. Xie, V. M. Burlakov, B. M. Henry, K. R. Kirov, H. E. Smith, C. R. M. Grovenor, H. E. Assender, G. A. D. Briggs, M. Kano, Y. Tsukahara, "Intensity-dependent relaxation of photoconductivity in nanocrystalline titania thin films", *Phys. Rev. B* **73**, 113317-1 to 113317-4 (2006).

[19] G. Marci, V. Augugliaro, M. J. López-Muñoz, C. Martín, L. Palmisano, V. Rives, m. Schiavello, R. J. D. Tilley, A. M. Venezia, "Preparation, characterization and photocatalytic activity of polycrystalline ZnO/TiO2 systems. 1. Surface and bulk characterization", *J. Phys. Chem. B* **105**, 1026-1032 (2001).